Quantum Monte Carlo evidence for *d*-wave pairing in the two-dimensional Hubbard model at a van Hove singularity

T. Husslein,* I. Morgenstern,* D. M. Newns, P. C. Pattnaik, J. M. Singer,* and H. G. Matuttis*
IBM Thomas J. Watson Research Center, P.O. Box 218, Yorktown Heights, New York 10598
(Received 16 October 1995; revised manuscript received 9 August 1996)

We implement a quantum Monte Carlo calculation for a repulsive Hubbard model with nearest- and next-nearest-neighbor hopping interactions on clusters up to 12×12. A parameter region where the Fermi level lies close to the van Hove singularity at the saddle points in the bulk band structure is investigated. A pairing tendency in the $d_{x^2-y^2}$ symmetry channel, but no other channel, is found. Estimates of the effective pairing interaction show that it is close to the value required for a 40 K superconductor. Finite-size scaling compares with the attractive Hubbard model.[S0163-1829(96)03646-6]

The two-dimensional (2D) Hubbard model (HM) contains several basic elements of the high-temperature superconductivity problem, and its properties include nontrivial features (e.g. the Mott transition and associated antiferromagnetism) which are generic in high T_c materials. Is the HM also a superconductor, or does the superconductivity originate from extrinsic interactions or degrees of freedom? According to calculations[1,2] based on exchange of antiferromagnetic spin fluctuations (AFSF), the HM is a superconductor with $d_{x^2-y^2}$ order parameter symmetry (a symmetry consistent with several recent experimental measurements[3–5]). But on the contrary quantum Monte Carlo (QMC) calculations up to the present[6–9] have given negative or inconclusive results regarding superconductivity of the 2D HM.

In the present QMC study of a generalized HM (which includes next-nearest-neighbor hopping interactions as well as the usual nearest-neighbor ones), we present evidence for a superconducting tendency in the $d_{x^2-y^2}$ channel in large (up to 12×12) clusters, in qualitative agreement with the AFSF calculations. The results have been obtained close to the parameter region where the energy of the saddle points (SP) in the band structure lies close to the ''Fermi level'' in the cluster energy level structure, a choice motivated by the hypothesis,[10–12] van Hove scenario, that, in the continuum limit, superconductivity is enhanced by the van Hove density of states peak associated with the saddle points.

The SP feature may be incorporated into the Hubbard model within the metallic regime by introducing a next-nearest-neighbor interaction. This allows the SP to lie at the Fermi level at a doping of, say 15–25 %, while the insulating point, at which the antiferromagnetic instability occurs, lies at 0% doping. These features are characteristic of real cuprate materials.[13,14] It is in the former situation (15–25 % doping) that the model is found to support superconductivity.

The model is specified as follows:

$$H=-t\sum_{\langle ij\rangle\sigma} c_{i\sigma}^{+}c_{j\sigma}+t'\sum_{\langle\langle ij\rangle\rangle\sigma} c_{i\sigma}^{+}c_{j\sigma}+U\sum_{i} n_{i\uparrow}n_{i\downarrow}. \quad (1)$$

In Eq. (1), U is the repulsive on-site Coulomb interaction, t is the nearest-neighbor hopping integral ($\langle ij\rangle$ denotes nearest-neighbor interactions), t' is the next-nearest-neighbor hopping integral ($\langle\langle ij\rangle\rangle$ denotes next-nearest-neighbor interactions); t and t' are defined to be positive.

The noninteracting band structure of the tt' Hubbard model (1) has saddle points at energy $-4t'$, and at $k=(0,\pi)$ and $(\pi,0)$. If we take the hole doping x to be of order $x\approx t'$, then the saddle points in the noninteracting band structure lie near E_F (see Fig. 1). In the absence of t', the required doping would be zero, making the sample insulating. The electronic effective mass below the SP's is heavier than the mass above, the ratio being $(t+2t')/(t-2t')$. Photoemission data indeed show a large mass ratio.[13,14] The simulation of the tt' Hubbard model 1 is based on the projector Monte Carlo technique, using the ansatz for the ground state[7]

$$|\Psi_g\rangle=e^{\Theta H}|\Psi_0\rangle, \quad \Theta\to\infty, \quad (2)$$

where Θ is a projection parameter and $|\Psi_0\rangle$ a single determinant taken as the ground state of the noninteracting band structure of 1.

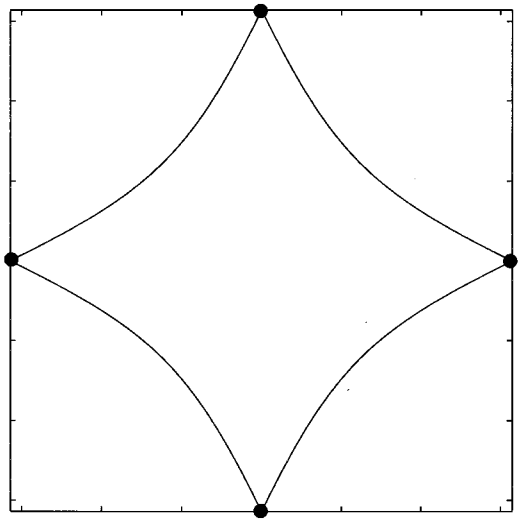

FIG. 1. Fermi surface of the noninteracting tt' Hubbard model $t'=0.3t$, $E_F=-1.2t$, hole doping=0.27. Solid circles indicate saddle points.

 © 1996 The American Physical Society

The exponent in Eq. (2) is broken up into Trotter slices on the interval Θ, and the Hirsch-Hubbard-Stratonovich[15] transformation applied to each slice, turning Eq. (2) into a path integral which is solved on a finite cluster (up to 12×12) using the Metropolis algorithm (for details see Ref. 7). We checked on the convergence of the algorithm by comparing small clusters to exact diagonalization and stochastic diagonalization[27] and found $\Theta=8$ and $\tau=0.125$ to be sufficient. Periodic boundary conditions and closed-shell configurations are always used. The ''average sign'' is usually sufficiently close to unity, that the simulations are not significantly limited by the fermionic sign problem. In a typical simulation we averaged over four runs with different seeds each run having at least 10^6 MCS. The nonexistence of a fermionic sign problem in the simulations and the very large number of MCS allowed us to obtain precise results for the superconducting correlation functions. The orthogonalization technique originally proposed by Sorella *et al.*[26] helped us to stabilize the algorithm. We found a stabilization every 8 Trotter slices to be sufficient to make the results independent of the number of stabilizations.

The tendency towards superconductivity is signaled[9,16] by the presence of a long-range ''plateau'' in the superconducting correlation ''function'' [9] plotted as a function of distance. Such plateaus have been demonstrated[7] in models such as the attractive Hubbard model and simplified models with electron-phonon coupling, where a pairing tendency is anticipated to occur. While studying finite systems one has always to extrapolate to the thermodynamic limit. Due to the unsystematic finite level structure of the finite Hubbard model this has turned out to be very difficult. We use two different approaches: (a) We are able to analyze the plateau in terms of the effective pairing interaction J, and hence deduce a value for T_c in the infinite-sample limit. (b) We find analogous finite-size scaling behavior for the superconducting correlations for the repulsive and the attractive Hubbard model.

The condition as to whether the finite cluster of size L is ''superconducting'' (correlation length $\xi>L$), or whether superconductivity is suppressed by finite size effects ($\xi<L$), does not enter into these considerations and is not relevant for this paper.

Some constraints on U are (a) according to exact diagonalization calculations the Hubbard model is an insulator at half-filling, as observed experimentally, if U is greater[17] than about $10t'$, (b) the value $U=2t$ has been used in calculations[18] of the quasiparticle lifetime broadening for the tt' Hubbard model in the renormalized propagator approximation, with results consistent with experimental data, (c) attempts to derive the single-band U formally from a multiband model[19] give a value of order 6 eV, i.e., $6t$, in the case $t=1$ eV. We have observed clear evidence for the superconducting tendency for U in the range $0.5t<U<3t$; for larger U values unacceptable error bars are obtained.

The superconducting correlation function $\chi(R_j)$ for $d_{x^2-y^2}$ symmetry is defined as

$$\chi(R_j)=\frac{1}{4N_L}\sum_i\sum_{\langle p\rangle,\langle q\rangle}\langle[c^+_{i\uparrow}c^+_{i+p\downarrow}-c^+_{i\downarrow}c^+_{i+p\uparrow}][c_{i+j+q\downarrow}c_{i+j\uparrow} -c_{i+j+q\uparrow}c_{i+j\downarrow}]\rangle\sigma_p\sigma_q-\chi_0(R_j), \tag{3}$$

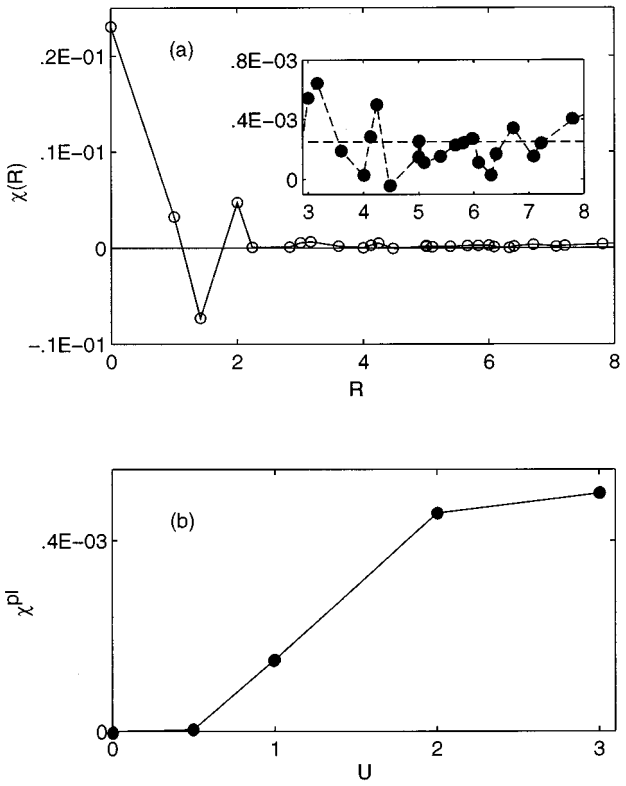

FIG. 2. (a) Superconducting vertex correlation function $\chi(R)$ [Eq. (3)], plotted vs distance R, 12×12 lattice, 106 electrons (doping 0.264), $\Theta=8/t$, $t'=0.286t$, $U=2t$. Inset shows correlation function on expanded scale, horizontal dashed line is average plateau value. Error bars are less than the width of the points. (b) QMC calculation of plateau vs U, for 8×8 lattice, 50 electrons (doping 0.22), $\Theta=8/t$, $t'=0.22$.

where

$$\chi_0(R_j)=\frac{1}{4N_L}\sum_{i,\sigma}\sum_{\langle p\rangle,\langle q\rangle}\{\langle c^+_{i\sigma}c_{i+j\sigma}\rangle\langle c^+_{i+p-\sigma}c_{i+j+q-\sigma}\rangle +\langle c^+_{i\sigma}c_{i+j+q\sigma}\rangle\langle c^+_{i+p-\sigma}c_{i+j-\sigma}\rangle\}\sigma_p\sigma_q.$$

Here, $\langle p\rangle$ implies a sum over nearest neighbors of 0, $p=(\pm1,0)$ and $(0,\pm1)$, for which σ_p is, respectively, 1 and -1, N_L is the number of atoms in the cluster, and σ is spin.

A typical calculation of the superconducting correlation function (3) for a (12×12) cluster is illustrated in Fig. 2(a). It is seen that, as a function of increasing distance, the correlation function in this symmetry approaches a ''plateau.'' It is only in $d_{x^2-y^2}$ symmetry that we find this behavior. The error bars in the points, calculated as the deviation between runs with different seeds, are smaller than their diameter.

A study of the variation of $\chi^{\rm pl}$ with U is shown in Fig. 2(b), based on 8×8 clusters. $\chi^{\rm pl}$ is seen to increase with U, and continues to increase steadily up to the largest value of $U(U=3t)$ for which we have adequate statistics.

The main problem with scaling our results is the influence of finite shell structure on the observables and the unsystematic behavior of these shells with system size. Therefore the application of finite-size scaling especially for weak U is

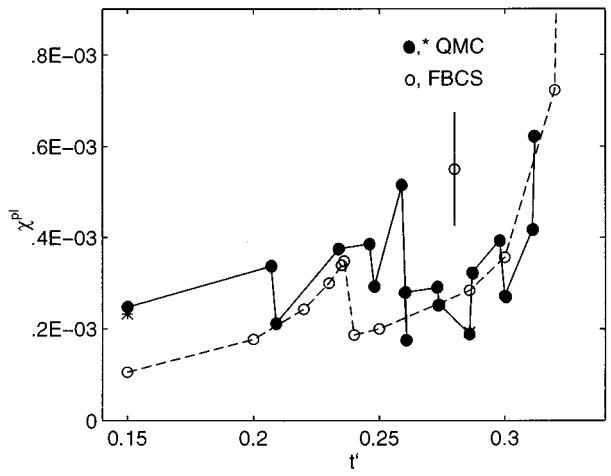

FIG. 3. Filled points QMC calculation of plateau value χ^{pl} of superconducting vertex correlation function [Eq. (3)] vs t', for 10×10 lattice, 74 electrons (doping 0.26), $\Theta=8/t$, $U=2t$, error bar is average; open points fbcs calculation [Eq. (4)] with $J=0.055t$ and cutoff $\omega_c=0.2t$.

extremely complex, as has already been observed for the case of the attractive Hubbard model.[24,25]

In Fig. 3 we illustrate a plot of the value of $\chi(R)$ averaged over the plateau region, χ^{pl}, versus t' for a 10×10 cluster with $N_e=74$ electrons. Each point in Fig. 3 represents a run with several different seeds, typically 4. Figure 3 contains points calculated using two different sampling algorithms, which are seen to agree quite well. The strong variation of χ^{pl} with t' seen in Fig. 3 is systematic, and is due to the shell structure of the cluster. The peaks in χ^{pl} are found to be associated with the near degeneracy of several filled and empty cluster levels, i.e., a high ''density of states at E_F.'' The dips in χ^{pl} coincide with regions of maximum gap in the single particle spectrum of the cluster between the highest occupied and lowest unoccupied levels.

A more quantitative analysis of the effect of shell structure on pairing is possible by introducing a simple low-energy pairing Hamiltonian[20]

$$H_p\sum_{k\sigma}\ \varepsilon_k n_{k\sigma}+J\sum_{k\neq k'}\ p_k^{+}p_{-k'},\eta_k\eta_{-k'}\,. \tag{4}$$

Here $k=a$ discrete wave vector for the cluster (periodic boundary conditions assumed) lying within the cutoff $|\epsilon_k-\mu|<\omega_c$, $p_k^{+}=c_{k\uparrow}^{+}c_{-k\downarrow}^{+}$, $\eta_k=[\cos(k_x)-\cos(k_y)]$, and J, which is negative, is a nearest-neighbor attractive interaction which parametrizes the pairing strength in the model (4).

For the present purpose we exploit the cutoff $|\epsilon_k-\mu|<\omega_c$, to solve Eq. (4) by exact diagonalization for states within ω_c. Having available the exact system ground state we can calculate χ^{pl}, which is also illustrated in Fig. 3 for $J=0.055t$. It is seen that the low energy Hamiltonian (4), with its shell-structure effects, well reproduces the corresponding structure in the QMC results. Using the complete eigenvalue and eigenvector spectrum of the H_p, within the cutoff, the projector formula for χ^{pl}, Eq. (2), can be evaluated explicitly for a given Θ; we find that the value $\Theta=1/8t$ adequately reproduces the ground state value of χ^{pl}.

TABLE I. Scaling $t'=0.22t$, $U=2t$.

N_L	N_e	ω_c	χ^{pl}	J
36	26	0.3 t	1.377×10^{-3}	0.12 t
64	50	0.25 t	0.648×10^{-3}	0.15 t
100	82	0.25 t	0.491×10^{-3}	0.15 t
144	122	0.25 t	0.332×10^{-3}	0.15 t

In Table I we demonstrate a possible technique for scaling QMC χ^{pl} data on different cluster sizes. The problem is to avoid the pronounced cluster shell-structure effects (Fig. 3). The technique is to compare J, obtained by fitting the Eq. (4) model to χ^{pl} at each cluster size, rather than χ^{pl}, for different sizes, whereby the shell-structure effects are taken into account. Values of J deduced from QMC calculations on $n\times n$ clusters with n from 6 to 12 are given in Table I. It is seen that the results appear to be converging on $J=-0.15t$, though results on a wider dynamic range of cluster sizes are needed to be convincing that convergence on the bulk limit has been achieved.

The foregoing method of analysis is extensible to include the case of a constant Z factor (Eliashberg notation). The analysis yields J/Z^2. A constant DOS ρ_0 renormalizes to $Z\rho_0$, giving $Z/(J\rho_0)$ in the exponent of the the T_c equation, which is the correct form and hence does not require any additional correction for Z. It is therefore valid, to within the constant-Z approximation, to proceed as if in the BCS case ($Z=1$). The largest value of J we have found is in the case $t'=0.22$, $U=3$ (see inset Fig. 3), for which $J=-0.2t$. This value of J is close to that ($J=-0.22t$) required to give a 40 K T_c, with $t=1$ eV.

In Fig. 4 we present a second method to extrapolate the data. We found in agreement with Ref. 24 that scaling laws of the form $1/N$ are too simple and can lead to ambiguous results. Instead of incorporating corrections to scaling while applying the scaling laws[27] we directly compare the results on $\chi^{\mathrm{pl}}_{d_{x^2-y^2}}$ for positive U with results on $\chi^{\mathrm{pl}}_{s_{os}}$ for negative U. In both cases we use the same system sizes, fillings, and t'. Hence the finite-size structure is identical. Additionally we use a value of $U=-0.3$ to match the size of the plateaus for

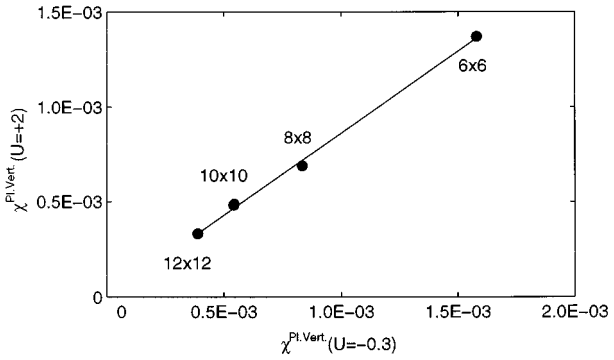

FIG. 4. Superconducting vertex correlation χ^{pl} in the onsite-s channel for attractive $U=-0.3$ vs superconducting vertex correlation χ^{pl} in the $d_{x^2-y^3}$ channel for the repulsive Hubbard model ($U=2$). Filling and t' are the same for both values of U and are indicated in Table I.

the positive $U(d_{x^2-y^2})$ case. Our analysis shows that the attractive and repulsive HM have the same scaling behavior. As the attractive HM is superconducting we conclude from the above that the repulsive HM is also superconducting.

Further light on the mechanism of pairing in the HM comes from an independent study of the Hubbard model based on the Roth decoupling procedure.[21,22] This study shows pairing of $d_{x^2-y^2}$ symmetry, and exhibits a clear correlation between pairing and nearest-neighbor spin correlation. Therefore the source of the pairing is probably a nearest-neighbor antiferromagnetic exchange interaction, generated by higher-order diagrams[23] in U, starting at U^2.

In conclusion, pairing correlations in $d_{x^2-y^2}$ symmetry, but no other symmetry, are found for the clusters and parameters studied in this paper. We presented two different ways of extrapolating our data to the thermodynamic limit. The tt' HM phase diagram thus includes the Mott transition, marginal Fermi-liquid behavior, and superconductivity, all the key features present qualitatively in real cuprates. The pairing interaction found in the parameter space explored so far supports a T_c of order 40 K. Full understanding of high-temperature superconductivity, including the highest T_c's, probably requires consideration of additional interactions, such as superexchange from the oxygen bands and mediation by phonons.

The Monte Carlo simulation was carried out on the IBM SP1. Typically the simulation at a single parameter occupied 4 processors for 80 h.

ACKNOWLEDGMENTS

Part of this work was supported by the Bayerische Forschungsverbund FORSUPRA. We are grateful to Joefon Jann for assistance with parallelization, and to K. A. Müller, D. J. Scalapino, and C. C. Tsuei for valuable discussions.

*Permanent address: Fakultät Physik, Universität Regensburg, D-930-53 Regensburg, Germany.

[1] X. Monthoux and D. Pines, Phys. Rev. Lett. **69**, 961 (1992); Phys. Rev. B **49**, 4261 (1994).
[2] X. Monthoux and D. J. Scalapino, Phys. Rev. Lett. **72**, 1874 (1994); D. J. Scalapino, Physica C **185–189**, 104 (1991).
[3] C. Tsuei *et al.*, Phys. Rev. Lett. **73**, 593 (1994); J. R. Kirtley *et al.*, Nature **373**, 225 (1995).
[4] L. N. Vu *et al.*, Appl. Phys. Lett. **63**, 1693 (1993).
[5] J. E. Sonier *et al.*, Phys. Rev. Lett. **72**, 744 (1993); M. Takigawa, J. L. Smith, and W. L. Hults, Phys. Rev. B **44**, 7764 (1991); M. Takigawa and D. B. Mitzi (unpublished).
[6] M. Imada, Physica C **185–189**, 1447 (1991); N. Furukawa and M. Imada, J. Phys. Soc. Jpn. **61**, 3331 (1992); R. R. dos Santos, Phys. Rev. B **39**, 7259 (1989); A. F. Veilleux *et al.*, *ibid.* **52**, 16 255 (1995).
[7] W. von der Linden, Phys. Rep. **220**, 55 (1992).
[8] A. Moreo, Phys. Rev. B **45**, 5059 (1992).
[9] S. R. White *et al.*, Phys. Rev. B **39**, 839 (1989).
[10] J. Labbe and J. Bok, Europhys. Lett. **3**, 1225 (1987).
[11] R. S. Markiewicz, Physica C **217**, 381 (1993), and references therein.
[12] D. M. Newns *et al.*, Comments Condens. Matter Phys. **15**, 273 (1992); P. C. Pattnaik *et al.*, Phys. Rev. B **45**, 5714 (1992); D. M. Newns *et al.*, Phys. Rev. Lett. **73**, 1695 (1994); D. M. Newns *et al.* (unpublished).
[13] D. M. King *et al.*, Phys. Rev. Lett. **73**, 3298 (1994); D. S. Dessau *et al.*, *ibid.* **71**, 2781 (1993); D. M. King *et al.*, *ibid.* **70**, 3159 (1993).
[14] K. Gofron *et al.*, Phys. Rev. Lett. **73**, 3302 (1994); A. A. Abrikosov, J. C. Campuzano, and K. Gofron, Physica C **73**, 214 (1993).
[15] J. E. Hirsch, Phys. Rev. B **31**, 4403 (1985).
[16] C. N. Yang, Rev. Mod. Phys. **34**, 694 (1962).
[17] W. Fettes, I. Morgenstern, T. Husslein, H.-G. Matuttis, J. M. Singer, and C. Baur, J. Phys. France **5**, 455 (1995).
[18] J. W. Serene and D. W. Hess, *Recent Progress in Many-Body Theories*, edited by T. L. Ainsworth, C. E. Campbell, B. E. Clements, and E. Krotscheck (Plenum, New York, 1992), Vol. 3, p. 469.
[19] H.-B. Schuttler and A. J. Fedro, Phys. Rev. B **45**, 7588 (1992).
[20] J. Wheatley and T. Xiang, Solid State Commun. **88**, 593 (1993).
[21] J. Rossat-Mignod *et al.*, Physica B **186-188**, 1 (1993); T. E. Mason *et al.*, Phys. Rev. Lett. **71**, 919 (1993); S.-W. Cheong *et al.*, *ibid.* **67**, 1791 (1993).
[22] J. Beenen and D. M. Edwards (unpublished).
[23] A. Kampf and J. R. Schrieffer, Phys. Rev. B **41**, 6399 (1990).
[24] E. Y. Loh, Jr. and J. E. Gubernatis, *Electronic Phase Transitions*, edited by W. Hanke and Yu. V. Kopaev (North-Holland, Amsterdam, 1989).
[25] H. de Raedt and M. Frick, Phys. Rep. **231**, 107 (1992).
[26] S. Sorella, S. Baroni, R. Car, and M. Parinello, Europhysics Lett. **8**, 663 (1989).
[27] T. Husslein, W. Fettes, and I. Morgenstern (unpublished).